

The procedure of deconvolution of design-accelerogram in 2D time-domain FEM analysis

La procédure de déconvolution de l'accélérogramme calculatoire dans l'analyse du type FEM en domaine temporel en 2D

A. P. Korzec

Institute of Hydro-Engineering/Polish Academy of Sciences, Gdańsk, Poland

ABSTRACT: The article presents the procedure for determining the input seismic loading used in the numerical modelling of the time-domain dynamic response of the earth dam located on a deformable soil layer. Such an operation is commonly called the signal deconvolution. The method being analysed is based on the signal theory for a time-invariant linear system, which assumes the existence of the transfer function of the analysed dynamic system. The transfer function of the model is derived based on a response of the model to the testing input motion. Then, it is used to transform the design surface accelerometric signal to the boundary condition of the discrete model. The hypothesis has been made that deconvolution procedure can be used for 2D nonlinear time-domain finite element analyses if the specific testing signal is used. The paper covers an elementary example of the elastic soil layer used to verify the procedure correctness and presents the numerical experiments carried out for a nonlinear material model of soil layer, which have examined the effect of the testing signal on the accuracy of the reproduced design-accelerogram. In the paper, the measures of the signal reproduction accuracy have been proposed. The results have revealed that for the Mohr-Coulomb and Hardening Soil with small strain stiffness models the most precise reproduction of the design-accelerogram is gained for the target signal with peak value reduced by 40%.

RÉSUMÉ: Cet article présente la procédure utilisée pour déterminer la charge sismique en entrée pour la modélisation numérique de la réponse dynamique en temps du barrage en terre situé sur une couche de sol déformable. Cette opération est communément appelée la déconvolution du signal. La méthode en cours d'analyse est basée sur la théorie du signal pour un système linéaire invariant dans le temps, qui suppose l'existence de la fonction de transfert du système dynamique analysé. La fonction de transfert du modèle est dérivée sur la base d'une réponse du modèle pour tester le mouvement d'entrée. Ensuite, il est utilisé pour transformer le signal accélérométrique de la surface de conception en la condition limite du modèle discret. L'hypothèse a été faite que la procédure de déconvolution peut être utilisée pour des analyses d'éléments finis 2D non-linéaires dans le domaine temporel si le signal de test spécifique est utilisé. Le document couvre un exemple élémentaire de couche de sol élastique utilisé pour vérifier l'exactitude de la procédure. Le document couvre aussi des expériences numériques effectuées pour un modèle de matériau de couche de sol non-linéaire qui ont été effectuées pour examiner l'effet du signal de test sur la précision de l'accélérogramme de conception reproduit. Dans le document, les mesures de la précision de reproduction du signal ont été proposées. Les résultats ont révélé que pour le modèle Mohr-Coulomb et Hardening Soil with small strain stiffness, la reproduction la plus précise de l'accélérogramme de conception est obtenue pour un signal cible avec une valeur de crête réduite de 40%.

Keywords: strong-motion record; deconvolution; dynamic response; finite element; time-domain; earth dam

1 INTRODUCTION

The aim of this paper is to examine the proposed procedure of determination of a seismic input boundary condition which is an essential element of stability assessment of an earth dam built on a deformable subsoil layer using finite element method.

Two-dimensional finite element analyses are conducted in a plain strain condition, (Figure 1, Figure 2). The base of the model is assumed to be rigid. For the sake of simplicity, the paper is focused on uniform horizontal excitation only. Dynamic loading is defined by several surface accelerograms with the designed peak value $A_H^D(t)$. The uniform seismic excitation $a_{bx}(t)$, is applied at the base of the FEM model. The seismic input is determined by the deconvolution procedure.

Three main groups of the deconvolution procedures can be distinguished. The most common is the one-dimensional deconvolution performed in the frequency domain (Ordóñez 2011). The deconvolution is conducted for an arbitrarily selected 1D soil profile (marked in Figure 2), neglecting the geotechnical complexity of a subsoil. The next two groups of methods are based on the dynamic properties of the very same FEM model used for the stability assessment. Therefore, the heterogeneity and nonlinearity of soil, topographic effects, and also the impact of structures are taken into account. The second group covers the iterative deconvolution techniques. The correction coefficients applied to seismic input are determined e.g. as the ratio of

the target and reproduced spectral density for each frequency (Sooch and Bagchi 2012). The third group is based on a transmittance function H , which describes the wave transformation between selected points in the FEM model. The transmittance function is determined in a preliminary calculation based on the model response to the testing input motion. The methods incorporate the different definition of the transfer function, e.g. the ratio of power spectral density of in- and output signal to power spectral density of the input signal (Dulińska 2012).

The article analyzes the method belonging to the third group. First, the main features of this method are discussed. Then, the accuracy of the signal reproduction is investigated. The impact of a reference point location on stability assessment is also discussed.

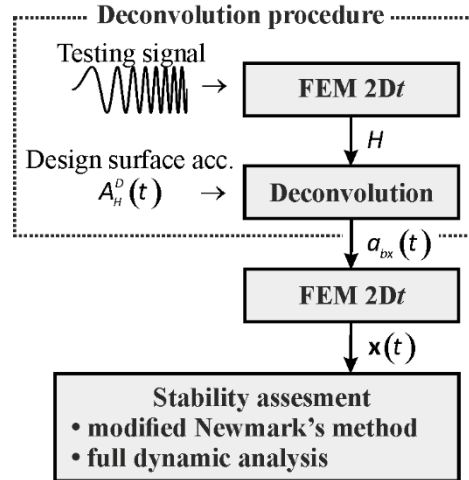


Figure 1. Stability assessment procedure using FEM

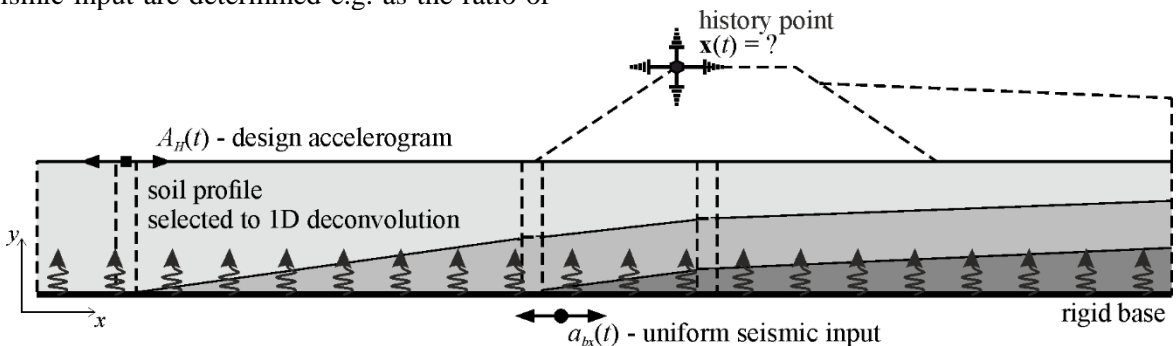


Figure 2. Sketch of the problem considered

2 DECONVOLUTION PROCEDURE

The considered method is based on the signal theory for the time-invariant linear system, Figure 1. It assumes the existence of the time-independent transmittance function of the analysed dynamic system $H(z)$, which describes the response of the dynamic system resulting from the excitation only.

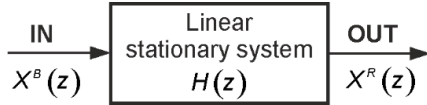


Figure 3. Deconvolution scheme

The transmittance function, also called transfer function, characterizes the properties of the system and describes how the amplitudes and phase shifts of all harmonic components are altered by the system. In the paper, the transfer function is defined as the ratio of input acceleration time-history to acceleration time-history calculated at the reference point after transforming both of the signals into the frequency domain

$$H(z) = \frac{X^R(z)}{X^B(z)} \quad (1)$$

where $X^R(z)$, $X^B(z)$ denotes the Fourier spectrum of horizontal seismic motion calculated on the subsoil surface and applied to the base of the model, respectively (Bendat and Piersol 1976).

The amplification function $|H(f)|$ and the phase shift function $\phi_0(f)$ are calculated as absolute value and argument of the transfer function

$$H(f) = \frac{1}{\cos\left(2 \cdot \pi \cdot f \cdot \frac{H}{V_S}\right) \cdot (1+i \cdot \eta)} \quad (2)$$

where f denotes a frequency (Hz), V_S is a shear wave velocity (m/s) (Kramer 1996). The example of $|H(f)|$ and $\phi_0(f)$, characterising the wave transformation in linear elastic 50 m thick soil layer (H) with 5% damping ratio (η), are shown in Figure 4 and Figure 5, respectively.

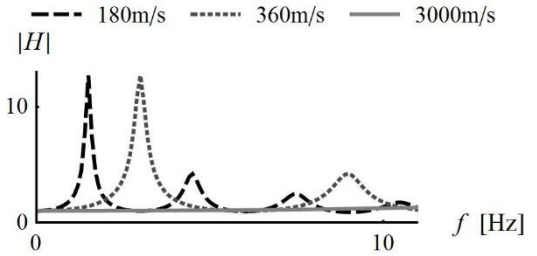


Figure 4. Amplification function of elastic soil layer for different shear wave velocity ($H = 50$ m, $\eta = 5\%$)

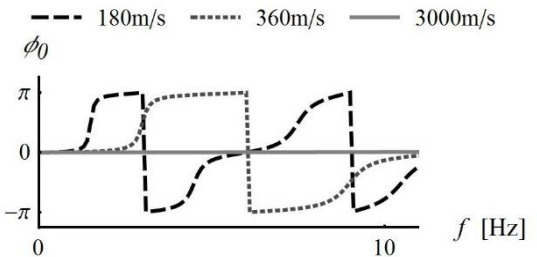


Figure 5. Phase shift function of elastic soil layer for different shear wave velocity ($H = 50$ m, $\eta = 5\%$)

The linear model of soil response is not accurate for strong excitation. An equivalent-linear model or nonlinear model should be routinely used for soil-structure interaction analysis. Therefore, the application of the above deconvolution procedure for the earthquake engineering purpose should be tested.

3 THE MEASURE OF ACCURACY

In the paper, the characteristic parameters of accelerogram were selected in order to confirm the correctness of the applied input seismic motion. The relative error of the peak value of the acceleration δp_a was assessed according to the (Equation 2). However, the accuracy of the signal reproduction should comprise the entire signal. Therefore, the relative error of Arias Intensity δI_a (Equation 4) was calculated as a measure of energy accuracy. Moreover, the weighted mean value of the relative errors of the amplitudes spectrum R_a (Equation 5) was proposed as a measure of accuracy.

$$\delta p_a = \frac{|p_a^{rec} - p_a^{calc}|}{p_a^{rec}} \cdot 100 \quad (3)$$

$$\delta I_a = \frac{|I_a^{rec} - I_a^{calc}|}{I_a^{rec}} \cdot 100 \quad (4)$$

$$R_a = \frac{\sum_i |F_{at}^{rec} - F_{at}^{calc}| \cdot 100}{\sum_i F_{at}^{rec}} \quad (5)$$

where i denotes subsequent frequencies.

4 DESIGN-ACCELEROGRAMS

The presented results were obtained for two horizontal accelerograms downloaded from European Strong-motion Database (ESD 2015). Both signals were recorded in the close epicentral distance of 4 km and 12 km, respectively. The moment magnitudes of earthquakes were 4.9 and 4.6, respectively. Both seismic stations are located in Italy on alluvial deposits.

The signals were firstly modified (Boore and Bommer 2005, Korzec and Świdziński 2018). First, the low-frequency noise was reduced. Then, the 5th-order low pass Butterworth filter was applied with a cut-off frequency of 10 Hz in order to reduce computational effort. Lastly, the signals were scaled up to the design peak horizontal acceleration PHA , e.g. equal 0.1g.

The modified accelerograms are shown in Figure 6 and Figure 7. The Fourier amplitudes spectrums are shown in the section of calculation results (see Figure 13 and Figure 15).

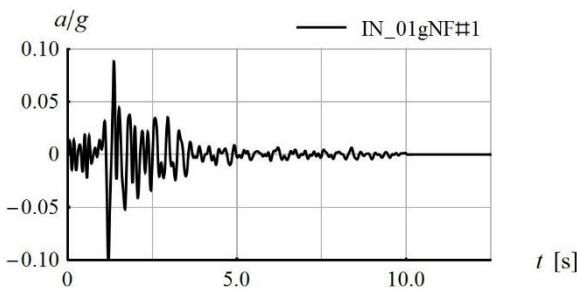


Figure 6. Modified Italy 1976 horizontal acceleration time-history (NF#1)

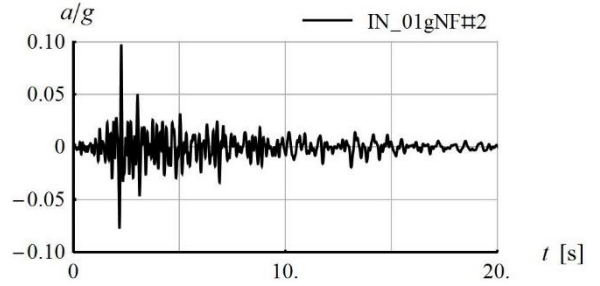


Figure 7. Modified Italy 1972 horizontal acceleration time-history (NF#2)

5 TESTING SIGNAL

Monoharmonic signals with different frequencies and obviously the design surface accelerogram were used as testing signals. The *linear chirp* was also used, which introduces subsequent frequencies in successive time steps with the rate of the frequency change equal to 2 (shown in Figure 1). The testing signal duration was at least 10 s.

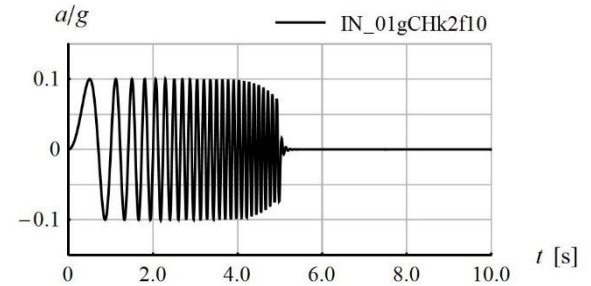


Figure 8. Linear chirp used as a testing signal

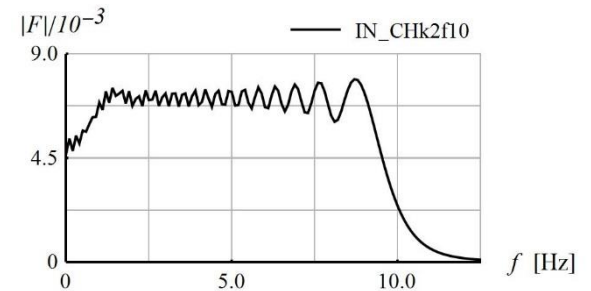


Figure 9. Fourier amplitudes spectrum of linear chirp used as a testing signal

6 NUMERICAL RESULTS

The presented calculations were performed in the commercial finite element program *PLAXIS* 2D. The triangular 6 nodes elements were used to model the finite medium. The distance between the nodes results from the assumption of the shortest wave description by at least 7 nodes. The direct Newmark's time-integration algorithm implemented in *PLAXIS* is used with constant average acceleration. The numerical damping is not introduced. The calculation step, calculated by very restrictive formula implemented in *PLAXIS* 2D 2012, satisfies both Nyquist and Courant conditions.

The mass and stiffness proportional Rayleigh damping model is implemented in *PLAXIS*. The reference frequencies (f_1 and f_2) of specified damping ratio were selected to gain the quite flat function of damping ratio in the range of 1÷10 Hz in order to decrease the damping dependency on a frequency.

The viscous absorbent elements are applied on both vertical boundaries of limited soil layer to minimize the reflection of waves back to the model. Moreover, the model width was 10 times its height.

6.1 Elementary example – elastic soil layer

As a basic example of deconvolution procedure, a uniform 50 m thick elastic soil layer, with the shear wave velocity V_S of 300 m/s and the soil damping ratio of 5% ($f_1 = 1.3$ Hz; $f_2 = 6.6$ Hz), was selected. The soil weight γ is 18 kN/m³. The small strain shear modulus G_0 calculated based on V_S and γ is equal to 165 MPa. The value of Poisson's ratio is 0.2. The nodal distance in the direction of propagating wave is 2 m and calculations are conducted with time increment equal 0.00125 s. The results are saved every 0.005 s.

The comparisons of theoretical and calculated amplification function and phase shift function, shown in Figure 10 and Figure 11, are in a good agreement. The discrepancies between the

calculated amplitudes result mostly from the incorporated damping model. The accuracy of the phase shift function seems to decrease for frequencies lower than the frequency of the longest standing wave ($f < 6$ Hz).

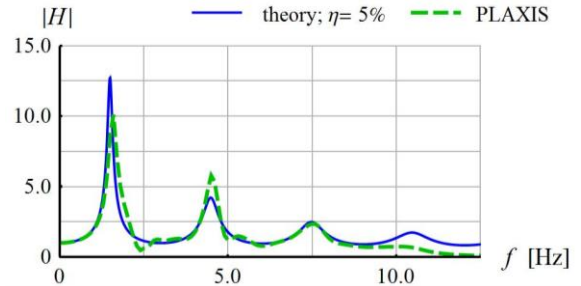


Figure 10. Comparison of theoretical amplitudes spectrum of elastic soil layer with calculated one using signal NF#1

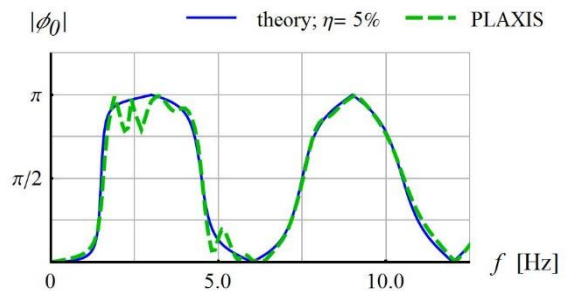


Figure 11. Comparison of theoretical phase shift function of elastic soil layer with calculated one using input seismic signal NF#1

The selected design-accelerograms were successfully reproduced at the reference point for four types of testing signals used in the deconvolution procedure, Table 1. Therefore, the correctness of the procedure's implementation was demonstrated. The most accurate results were obtained for the target signal, however, the very good agreement was also obtained for the *chirp*-type signal. It is a very important conclusion, having in mind that the stability assessment should be performed on the basis of at least three and preferably on the basis of ten independent, uncorrelated excitations.

The comparison of design and reproduced acceleration time-history *NF#1* and their spectra for the *chirp*-type testing signal are shown in

Figure 12 and Figure 13. The relative error of peak horizontal acceleration δpa value is 0.89%, and the Arias intensity relative error δIa is 0.46%.

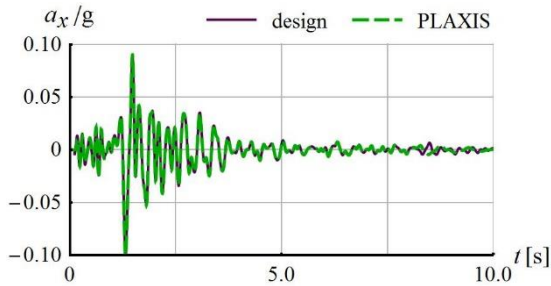


Figure 12. Comparison of design and reproduced acceleration time-history NF#1 at reference point using chirp signal as a testing signal

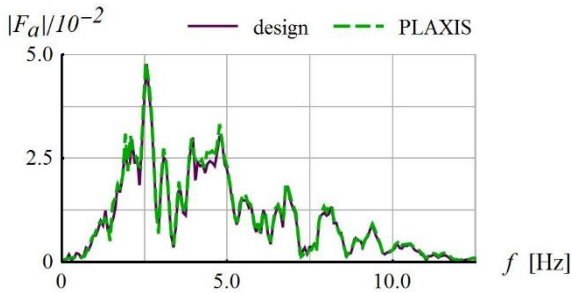


Figure 13. Fourier amplitudes spectra of design and reproduced acceleration time-histories NF#1 at reference point using chirp signal as a testing signal

Table 1. The accuracy measures of reproduction of design-accelerogram NF#1 at reference point determined for a different type of testing signals

T.signal	δpa [%]	δIa [%]	R_a [%]
monoCH	2.05	10.65	14.0
CH_k2f10	0.89	0.46	8.8
NF#1	0.33	0.47	8.6
NF#2	0.54	0.53	8.7

The distribution of relative error of acceleration amplitudes spectrum δF_a is shown in Figure 14. The largest value of δF_a occurred for relatively low wave's amplitudes. The weighted mean value of these errors, calculated within the frequency range of 0.1 Hz to 10 Hz, is equal to 8.8%. The dominant frequency of the analysed signal, equal to 2.59, was precisely reproduced

and the error of its amplitudes does not exceed 1.5% for all testing signals.

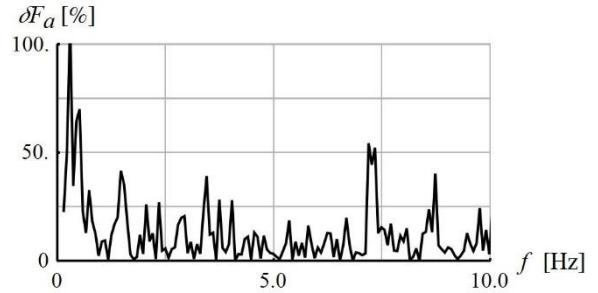


Figure 14. The relative errors of reproduced NF#1 Fourier amplitudes using chirp signal as a testing signal

In the case of the design-accelerogram NF#2, the weighted mean of relative errors of amplitudes spectrum takes a higher value equal to 23.4%. The comparison of the design and reproduced acceleration amplitudes' spectra for testing signal NF#2 is shown in Figure 15. However, the design-accelerogram can be considered accurately reproduced. The relative errors of accelerogram are δpa of 0.01% and δIa 1.35%.

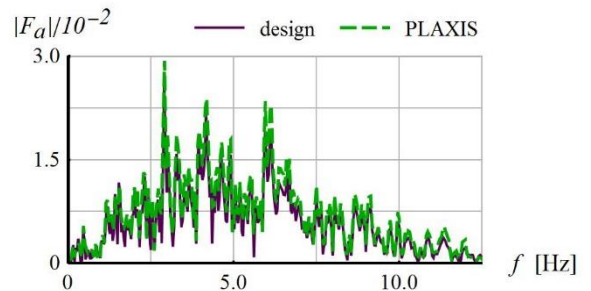


Figure 15. Fourier amplitudes spectra of design and reproduced NF#2 acceleration time-histories at reference point using NF#2 as a testing signal

6.2 Elastoplastic soil layer

The second example concerning the reproduction accuracy is the non-cohesive soil layer modelled by the elastoplastic Mohr-Columb material. The elastic parameters correspond to the above described elastic soil. The elastic modulus E' is 396.7 MPa. The assumed strength parameters

are: the effective friction angle of 30° , the dilatancy angle of 5° .

The comparison between amplification functions determined for the different peak values of the testing signal *NF#1* revealed its effect on the transfer function. Therefore, the appropriate peak value of the testing signal should be selected, which ensures good accuracy of the reproduced design-accelerogram, Figure 16. The high-frequency noise appeared in the calculation results of the non-linear analysis.

The design-accelerogram *NF#1* with relatively small peak value, within the range of 0.1g to 0.2g, were reproduced successfully for *chirp* and *NF#1* testing signals scaled to 0.1g. The relative error of the acceleration peak value δp_a was 0.45% and 0.3%, respectively. The weighted mean value of relative errors of acceleration amplitudes spectrum R_a , in both cases, was around 9%. Whereas, in the case of the higher peak value of design-accelerogram *NF#1*, equals to 0.6g, very good reproduction was achieved only for *NF#1*

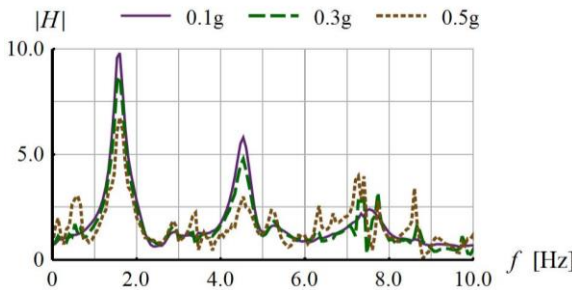


Figure 16. Comparison between amplification functions determined for scaled signal *NF#1*

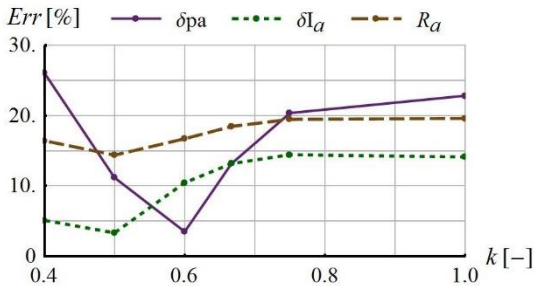


Figure 17. The errors of design-accelerogram reproduction at a reference point in the function of k (quotient of peak values of testing signal *NF#1* and design signal *NF#1*)

testing signal with around two times lower peak value, Figure 17. The reproduction errors for testing signal *NF#1* scaled to 0.3g were δp_a of 11.5%, δI_a of 3.3% and R_a of 14.4%. The highest relative error occurred for amplitudes close to the third natural frequency of the layer equal to 7.5 Hz, Figure 18.

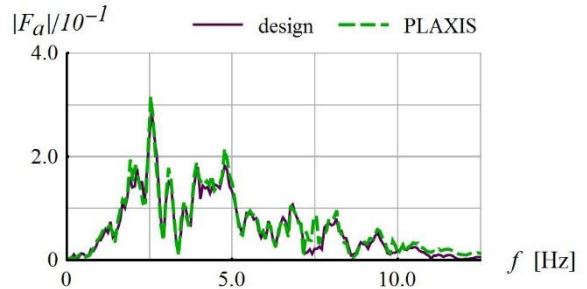


Figure 18. Fourier amplitudes spectra of design and reproduced 0.6g *NF#1* acceleration time-histories at reference point using target signal scaled to 0.3g as a testing signal

The use of a *chirp* signal, which causes the development of higher strains in the soil, requires much higher peak value reduction of the testing signal. Nevertheless, the frequencies close to the natural frequencies are overamplified. The reproduction errors achieved for 0.3g *chirp* signal were δp_a of 9%, δI_a of 44% and R_a of 35%.

6.3 The structure impact on seismic input determination

In a simplified approach to dynamic stability analysis (pseudo-static analysis, classic Newmark's method) the peak acceleration value or the design-accelerogram is applied to a rigid wedge. In the case of the 2D finite element analysis, two questions arise. First, at which point of the discrete model the design-accelerogram should be reproduced, and second, should the structure be included since the soil stiffness dependency on stress is well known.

A simplified model of the tailings dam was considered. The HSS model was used for all of the materials with dynamic parameters shown in Figure 19. The normalized stiffness reduction

curves were assumed based on the plasticity index and mean effective stress according to the formulation given in (Ishibashi and Zhang 1993). The design-accelerogram was reproduced at point R2 for the two cases: before (reference case) and after dam construction, called hereafter *free-field* and *structure*, respectively.

The peak values of shear stains $\gamma_d(t)$ and horizontal displacement $u_x(t)$ time-histories are compared in Table 2. The results unambiguously

indicate that dynamic response is significantly greater if the design-accelerogram is reproduced under the dam.

Table 2. Comparison of dam's dynamic response

Point	P1	P2	R3	R4
Case	$p\gamma_d$ (%)	$p\gamma_d$ (%)	pu_x (m)	pu_x (m)
free-field	5.5	3.9	0.080	0.087
structure	7.8	6.1	0.090	0.123
Δ (%)	41.8	56.4	12.5	41.4

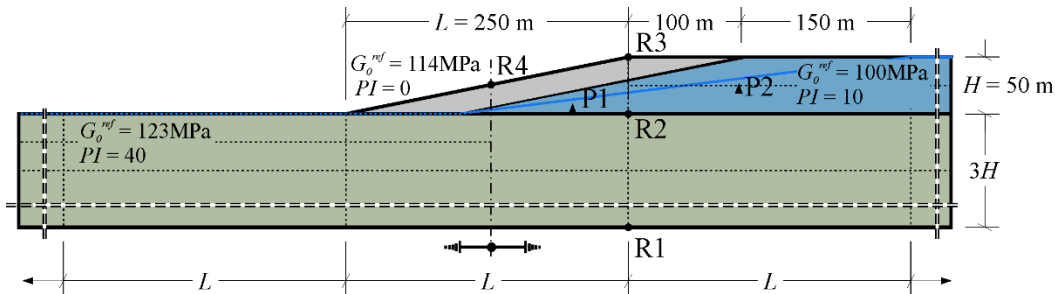


Figure 19. Simplified tailings dam model

7 CONCLUSIONS

The correctness of the presented deconvolution procedure was demonstrated. The presented deconvolution procedure can be used for 2D nonlinear time-domain finite element analyses if the specific testing signal is used.

The accuracy of the signal reproduction depends on the testing signal used to determine the transfer function. The *linear chirp*-type signal is recommended for cases of elastic dynamic response. Whereas, for the nonlinear response, the target signal with reduced peak value should be used as a testing signal. In cases analysed the reduction factor was 0.5÷0.6.

Generally, the seismic input determined using deconvolution procedure depends on the location of the point and surface load.

8 REFERENCES

Bendat, J.S., Piersol, A.G. 196. *Metody analizy i pomiaru sygnałów losowych*. Państwowe Wydawnictwo Naukowe, Warszawa.

Boore, D.M., Bommer, J.J. 2005. Processing of strong-motion accelerograms: needs, options and consequences. *Soil Dynamics and Earthquake Engineering* **25**: 93-115.

Dulinska, J. 2012. *Ziemne budowle hydrotechniczne na terenach sejsmicznych i para-sejsmicznych w Polsce. Wybrane aspekty modelowania*. Wydawnictwo Politechniki Krakowskiej, Kraków.

ESD. *Internet-Site for European Strong-motion Data* – <http://www.isesd.hi.is> (downloaded in 2015).

Ishibashi, I., Zhang, X. 1993. Unified dynamic shear moduli and damping ratios of sand and clay. *Soils and Foundations* **33** (1): 182-191.

Kramer, S.L. 1996. *Geotechnical Earthquake Engineering*, Prentice-Hall Inc.

Ordóñez, G.A. 2011. *SHAKE2000. A computer program for the 1-D analysis of geotechnical earthquake engineering problems. User's manual*. GeoMotions.

Sooch, G.S., Bagchi, A. 2012. Effect of seismic wave scattering on the response of dam-reservoir-foundation system. *Proceedings, 15th World Conference On Earthquake Engineering*, Portugal.